Admittance Properties of Electrodiffusion Membrane Models

MICHAEL C. MACKEY
Department of Physiology, McGill University, Montreal, Quebec, Canada.

Communicated by J. Jacquez

ABSTRACT

A small signal analysis of the single ion Nernst-Planck equation is carried out to determine the equivalent admittance of membrane ion penetration sites where only one ionic species may move through the site. In addition to the assumptions inherent in the Nernst-Planck formulation I assume that a spatially constant electric field exists within the membrane. The analysis shows that Nernst-Planck electrodiffusion systems display anomalous reactance properties qualitatively consistent with those found in the membrane of many excitable cells, and predicted by a small signal analysis of the Hodgkin-Huxley equations. A quantitative comparison between the results obtained and the small signal Hodgkin-Huxley expression appropriate for potassium current at the squid giant axon resting potential yields estimates of zero and infinite frequency conductances and the (anomalous) inductance that are within an order of magnitude of each other. This comparison also allows an estimate of the squid giant axon membrane potassium diffusion coefficient, $D_K \sim 7 \times 10^{-10}$ cm^2/sec at 6.3°C and a resting potential of -60 mV.

INTRODUCTION

Early attempts to characterize the electrical properties of excitable membranes utilized alternating current impedance measurements on the giant axon of *Loligo* and the excitable cell from *Nitella*. Transverse impedance measurements on both of these systems in the resting state gave data that were interpreted as arising from a membrane capacity (C_m) of approximately 1 μF/cm^2 in parallel with a membrane resistance (R_m) on the order of 10^3 ohm cm^2 [14, 11].

Further experiments, utilizing transverse impedance measurements during excitation in both *Nitella* and squid, conclusively demonstrated that the major change during an action potential was a transient decrease in R_m [9, 10]. In addition to this transient change in membrane resistance during

excitation, it was noted that there was a small but consistent change in the reactive component of the membrane impedance. The effect could always be interpreted as a decrease in membrane capacity, and was most pronounced during the falling phase of the action potential. Similar results were obtained during the passage of current through the membrane [7].

Cole and Baker [7], using longitudinal impedance measurements, were able to extend their *Loligo* axon membrane data to frequencies much lower than was possible with transverse measurements. Some interesting phenomena came to light at frequencies below 250 cps. In this frequency range there was a clear indication that the reactive components of the membrane impedance could, under some conditions, become inductive. The data indicated the existence of a membrane inductive element on the order of 0.2 H cm^2. Apparently, the impedance properties of the squid giant axon membrane derived from two different components. One, a high frequency region, always exhibited a capacitive reactance; while a second, low frequency, portion had a reactive element that was either capacitive or inductive. A number of experiments indicated that the low frequency reactive portion was likely to become inductive in lowered external calcium solutions or in high external potassium solution. Cole [3,4] hypothesized that the low frequency characteristics of the membrane impedance were associated with potassium movement across the excitable membrane. Oscillatory behavior, also indicative of the existence of a membrane inductive element, was noted by Hodgkin and Rushton [19] in a small signal time domain analysis on the giant axon of *Homarus*. Similar results were noted by Weidmann [26] in *Nitella*.

With the advent of the characterization and detailed analysis of excitable membrane behavior in the time domain [18], it became possible to understand the origin of the frequency dependent behavior noted earlier. A small signal analysis of the Hodgkin-Huxley equations about the resting potential leads to a frequency domain equivalent circuit representation for the excitable membrane [1,6]. This analysis indicates that at low frequencies the reactance of the membrane should be inductive, with the majority of the contribution coming from potassium conductance activation. A small amount of the inductance derives from sodium conductance inactivation. The reactive element of the sodium conductance activation is capacitive, so at higher frequencies the sodium channel exhibits a net capacitance.

Mauro, Conti, Dodge, and Schor [20] carried out a detailed experimental study of the small signal time domain electrical responses of the membrane of the giant axon of *Todarodes sagittatus*. They found excellent agreement between their results and the behavior predicted from a small signal analysis of the Hodgkin-Huxley equations.

These small signal results from the linearized Hodgkin-Huxley equations

allow a qualitative understanding of the phenomena mentioned earlier. It was noted that during excitation the membrane impedance does not behave as if there were a pure resistive decrease, but rather as if there were a change in reactance, and that the deviation from the ideal is maximal during the falling phase of the action potential. This may be accounted for by the inductive behavior of the potassium activation system and the capacitive behavior of the sodium activation system, respectively. Both of these effects would tend to increase the series reactance of the membrane, interpreted as a decrease in membrane capacitance.

It seems likely that the effects of elevated external potassium on membrane impedance are due to a decrease in membrane potential. The primary effect of this depolarization is to activate the potassium conductance, and thus to increase the apparent membrane inductance. The fact that the inductive effect decreases past a certain potassium concentration may be due to competitive effects of the sodium system. The effects of external calcium alterations admit of a similar explanation. Frankenhaeuser and Hodgkin [15] have shown that an increase in calcium affects the membrane much like a hyperpolarization, which would tend to remove the potassium system from activity, with an attendant inductive effect. The effects of low calcium concentrations are much like the effects of high external potassium concentrations and can be explained in the same fashion.

Although use of the linearized Hodgkin-Huxley equations gives qualitative insight into the ionic origin of the impedance properties noted in excitable systems, it gives little, if any, feeling for the mechanisms associated with ion transport that might give rise to inductive or capacitive effects.

In this paper I analyse the small-signal admittance properties of a membrane model system in which it is assumed that ions traversing the membrane obey the Nernst-Planck electrodiffusion equation [21–24]. Thus, the effects of ionic diffusion coefficients, equilibrium potentials, and the membrane potential in determining the reactive and resistive behavior of membrane transport elements may be evaluated.

The decision to base an analysis of this type on electrodiffusion theory was made on a twofold basis. Cole [6] has extensively reviewed the properties of excitable membrane systems and the attempts to model them. Although electrodiffusion theory, in the Nernst-Planck formulation, fails to explain or predict behavior contained in the full Hodgkin-Huxley formulation of axonal properties, it does offer considerable insight into subthreshold properties. Cohen and Cooley [2] and Cooley, Dodge, and Cohen [13] observed that electrodiffusion model systems display time domain computed responses suggestive of systems with mixed capacitive-inductive

reactance properties. These considerations, coupled with Sandblom's [25] computed frequency domain behavior in a linearized Nernst-Planck system, makes a general analytical study of anomalous reactance properties in electrodiffusion systems potentially interesting.

ANALYSIS

I assume that there exist discrete, spatially localized regions within the membrane through which ions move [17]. In this analysis the admittance properties of one class of ions moving through one type of ion permeable membrane region will be examined. It is assumed that the ions under consideration have a signed valence z, move in the $\bar{x}$ direction perpendicular to the membrane surface, and have a number density $\bar{N}$ which is a function of both $\bar{x}$ and time $\bar{t}$: $\bar{N}(\bar{x},\bar{t})$. Within the ion permeable regions of the membrane, the ions are characterized by a diffusion coefficient D (cm^2/sec) and mobility μ [(cm/sec)/joule/cm)]. There is a potential, $\bar{\varphi}(\bar{x},\bar{t})$ across the membrane. The ionic current density, $\bar{I}(amp/cm^2)$ is given by [21–24]

$$\bar{I}(\bar{x},\bar{t}) = -qD\left[\frac{\partial \bar{N}}{\partial \bar{x}} + \frac{q}{kT}\bar{N}\frac{\partial \bar{\varphi}}{\partial \bar{x}}\right], \tag{1}$$

where $q = ze$ (coulombs).

In addition to Eq. (1), the continuity equation is required:

$$\frac{\partial \bar{I}}{\partial \bar{x}} = -q\frac{\partial \bar{N}}{\partial \bar{t}} \tag{2}$$

To deal with Eqs. (1) and (2) a knowledge of $\bar{\varphi}(\bar{x},\bar{t})$ is needed; this is normally derived from Poisson's equation. However, in accord with much other work on electrodiffusion models, attention is directed here to situations satisfying the Goldman [16] constant field assumption.

It will prove convenient to deal with dimensionless variables, so let

$$\begin{aligned} x &= \bar{x}/d, & N &= \bar{N}/N_i, \\ t &= \bar{t}D/d^2, & \varphi &= \bar{\varphi}e/kT, \\ \omega &= \bar{\omega}d^2/D, & I &= \bar{I}d/eDN_i, \end{aligned} \tag{3}$$

where d is the thickness of the membrane, N_i is the intracellular ionic number density, and ω is the angular frequency. With the definitions of (3), Eqs. 1 and 2 become

$$I = -z\left[\frac{\partial N}{\partial x} + zN\frac{\partial \varphi}{\partial x}\right] \tag{4}$$

and

$$\frac{\partial I}{\partial x} = -z\frac{\partial N}{\partial t}, \tag{5}$$

respectively.

DETERMINATION OF THE MEMBRANE ADMITTANCE

The behavior of the electrodiffusion model for small perturbing time dependent voltages, $\delta\varphi \exp(-j\omega t)$ with $j = \sqrt{-1}$, about a steady state voltage φ_0 is of primary interest, so take

$$I(x,t) = I_0(x) + \delta i \exp(-j\omega t),$$

$$\varphi(x,t) = \varphi_0(x) + \delta\varphi \exp(-j\omega t),$$

$$N(x,t) = N_0(x) + \delta n \exp(-j\omega t).$$

When these relations are substituted into (4) and (5), two sets of equations are obtained. The first,

$$I_0 = -z\left[\frac{dN_0}{dx} + zN_0\frac{d\varphi_0}{dx}\right], \tag{6}$$

describes the steady state ion flow; while the second set,

$$\delta i = -z\left[\frac{d\delta n}{dx} + zN_0\frac{d\delta\varphi}{dx} + z\delta n\frac{d\varphi_0}{dx}\right] \tag{7}$$

and

$$\frac{d\delta i}{dx} = j\omega z\delta n, \tag{8}$$

describe the perturbed state.

Steady State. Utilizing the Goldman constant field assumption and referring the potential at the inner border of the membrane ($\varphi = \varphi_i$ at $x = 0$) to the potential at the outer membrane border ($\varphi = \varphi_d$ at $x = 1$), we have $\varphi_0(x) = \varphi_m(1-x)$, where $\varphi_m = \varphi_i - \varphi_d$. Thus $d\varphi_0/dx = -\varphi_m$, and (6) becomes

$$I_0 = -z\left[\frac{dN_0}{dx} - zN_0\varphi_m\right], \tag{9}$$

where the Einstein relation, $D=\mu kT$, has been used in writing (9). Given the boundary conditions $N_0=1$ (N_d) at $x=0$ (1), assumed to be experimentally maintained, the integration of (9) yields

$$N_0=\alpha\exp(z\varphi_m x)+\beta, \tag{10}$$

wherein

$$\alpha=\frac{1-N_d}{1-\exp z\varphi_m} \tag{11}$$

and

$$\beta=\frac{N_d-\exp z\varphi_m}{1-\exp z\varphi_m}. \tag{12}$$

$\varphi_e=z^{-1}\ln N_d$ is the ionic equilibrium potential.

Perturbed State. Again make the constant field assumption with respect to the perturbing voltage $\delta\varphi$, so $\delta\varphi=\delta\varphi_m(1-x)$ and (7) becomes

$$\delta i=-z\left[\frac{d\delta n}{dx}-zN_0\delta\varphi_m-z\varphi_m\delta n\right] \tag{13}$$

or, in conjunction with (8),

$$-j\omega\delta n=\frac{d^2\delta n}{dx^2}-z\delta\varphi_m\frac{dN_0}{dx}-z\varphi_m\frac{d\delta n}{dx}. \tag{14}$$

If the spatial Fourier transform of δn is denoted by $\tilde{n}(s,\omega)$ and (10) is used to calculate dN_0/dx, Eq. (14) may be solved for δn to give

$$\tilde{n}(s,\omega)=\frac{z^2\alpha\varphi_m\delta\varphi_m}{(s-z\varphi_m)[s(s-z\varphi_m)+j\omega]}. \tag{15}$$

Further denoting the Fourier transform of δi by $\tilde{i}(s,\omega)$,

$$\tilde{i}(s,\omega)=z^2\left[\frac{\beta\delta\varphi_m}{s}+\frac{\alpha\delta\varphi_m}{s-z\varphi_m}\right]-z(s-z\varphi_m)\tilde{n}(s,\omega) \tag{16}$$

results from (13).

If Eq. (15) for $\tilde{n}$ is substituted into (16) for $\tilde{i}$, the (spatial) Fourier transformed admittance, $\tilde{Y}(x,\omega)=\tilde{i}/\delta\varphi_m$, becomes

$$\tilde{Y}(s,\omega)=z^2\left[\frac{\beta}{s}+\frac{\alpha}{s-z\varphi_m}-\frac{\alpha z\varphi_m}{s(s-z\varphi_m)+j\omega}\right], \tag{17}$$

from Eq. (16).

Let the real and imaginary parts of $\tilde{Y}(s,\omega)$ be given by $\tilde{G}(s,\omega)$ and $\tilde{B}(s,\omega)$, respectively, so $\tilde{Y}(s,\omega)=\tilde{G}(s,\omega)+j\tilde{B}(s,\omega)$. Thus, from (17),

$$\tilde{G}(s,\omega)=z^2\left[\frac{\beta}{s}+\frac{\alpha}{s-z\varphi_m}-\frac{\alpha z\varphi_m s(s-z\varphi_m)}{s^2(s-\varphi_m z)^2+\omega^2}\right] \tag{18}$$

and

$$\tilde{B}(s,\omega)=\frac{\alpha z^3\varphi_m\omega}{s^2(s-z\varphi_m)^2+\omega^2}. \tag{19}$$

It is possible from (17), or from (18) and (19), to write an expression for $Y(x,\omega)$, or $G(x,\omega)$ and $B(x,\omega)$. However, the resulting expressions are so complicated that the essential features I wish to discuss are obscured.

THE BEHAVIOR OF THE TRANSFORMED MEMBRANE ADMITTANCE

Following Cole and Cole [8], it will be convenient to discuss the behavior of $\tilde{Y}(s,\omega)$ in the complex admittance plane, displaying $\tilde{B}(s,\omega)$ as a function of $\tilde{G}(s,\omega)$ with ω as a parametric variable.

From Eq. (18) it is easy to show that the transformed zero and infinite frequency conductances are given by

$$\tilde{G}_0(s)=\lim_{\omega\to 0}\tilde{G}(s,\omega)=\frac{z^2}{s} \tag{20}$$

and

$$\tilde{G}_\infty(s)=\lim_{\omega\to\infty}\tilde{G}(s,\omega)=z^2\left[\frac{\beta}{s}+\frac{\alpha}{s-z\varphi_m}\right], \tag{21}$$

respectively. Let

$$\tilde{G}_1(s)=\left[\tilde{G}_\infty(s)-\tilde{G}_0(s)\right]/2 \tag{22}$$

and

$$\tilde{G}_2(s)=\left[\tilde{G}_\infty(s)+\tilde{G}_0(s)\right]/2. \tag{23}$$

Then it is a simple matter to show that

$$\left[\tilde{G}(s,\omega)-\tilde{G}_2(s)\right]^2+\left[\tilde{B}(s,\omega)\right]^2=\left[\tilde{G}_1(s)\right]^2 \tag{24}$$

Thus, from Eq. 24, as ω ranges from $-\infty$ to $+\infty$, $\tilde{Y}(s,\omega)$ describes a circle

in the complex admittance plane of radius $\tilde{G}_1(s)$ with its center on the $\tilde{G}(s,\omega)$ axis at $\tilde{G}_2(s)$. Only non-negative frequencies are of interest, so for this range of ω the relationship is a semicircle. Further, from the requirements for the existence of the transforms in (18) and (19) and the expressions for α and β given in (11) and (12),

$$\left.\begin{array}{c} \tilde{G}_\infty(s)-\tilde{G}_0(s) \\ \dfrac{\partial \tilde{G}(s,\omega)}{\partial \omega} \\ \tilde{B}(s,\omega) \end{array}\right\} > 0 \ (<0)$$

if $z(\varphi_m-\varphi_e)>0$ (<0). From all of the above considerations the complex admittance plane behavior of $\tilde{Y}(s,\omega)$ is as illustrated in Fig. 1.

The total admittance of a circuit consisting of a conductance G_1 in parallel with a series combination of a conductance G_2 and a susceptance B may be written as

$$Y_T = G_1 + \frac{jBG_2}{G_2+jB},$$

or, upon separation into real and imaginary portions,

$$\mathrm{Re}[Y_T] = G_1 + \frac{G_2B^2}{G_2^2+B^2}$$

and

$$\mathrm{Im}[Y_T] = \frac{G_2^2B}{G_2^2+B^2}.$$

The susceptance of a pure capacitance is $B=\omega C$, while for an inductance $B=-(\omega L)^{-1}$; therefore, comparison of the circuit equations from Fig. 2 with equations 11 and 12 immediately leads to the identification of $\tilde{G}_\infty(s)$ with G_1, $\tilde{G}_\infty(s)-\tilde{G}_0(s)$ with G_2, and B with a capacitor $C=\alpha z^3\varphi_m/\omega^2$ when $\tilde{B}(s,\omega)$ is positive and with an inductor $L=-(\alpha z^3\varphi_m)^{-1}>0$ when $\tilde{B}(s,\omega)$ is negative. Thus, the admittance plane properties of Fig. 1 may be completely derived from the equivalent electrical circuit representations shown in Fig. 2.

Therefore, any ion transport system described by the Nernst-Planck electrodiffusion equations with constant electric field will display "anomalous reactance" properties if there is an ionic concentration gradient across the membrane and the membrane potential φ_m is not identical to the ionic equilibrium potential φ_e. In a tissue such as the squid giant axon, with normal intra- and extracellular environments, the analysis of this simple

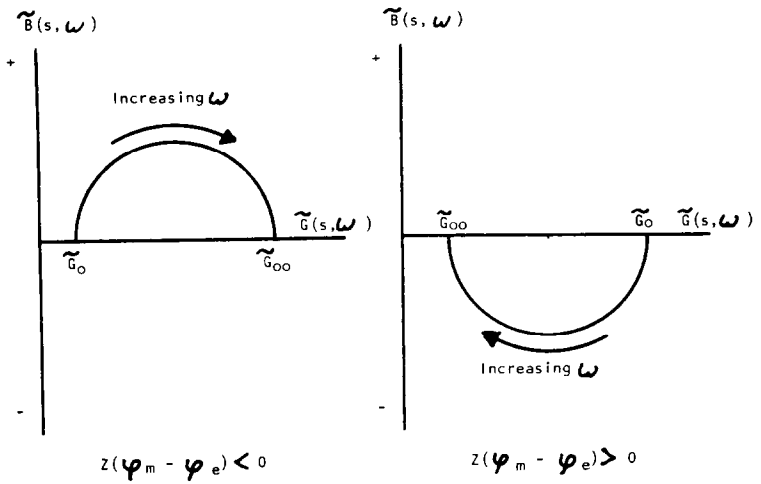

FIG. 1. The behavior of the (spatially) Fourier transformed admittance $\tilde{Y}(s,\omega) = \tilde{G}(s,\omega) + j\tilde{B}(s,\omega)$, obtained from a small signal analysis of the Nernst-Planck single ion equation and the continuity equation. Susceptance, $\tilde{B}(s,\omega)$, is shown as a function of conductance, $\tilde{G}(s,\omega)$, with ω as a parametric variable. $\tilde{G}_0$ and $\tilde{G}_\infty$ are, respectively, the zero and "infinite" frequency conductances and are given by Eqs. 20 and 21. A positive susceptance corresponds to a capacitance, negative to an inductance. The left hand plot shows the admittance plane behavior for $z(\varphi_m - \varphi_e) < 0$, where z is the ionic valence and φ_m and φ_e are the membrane and ionic equilibrium potentials, respectively. On the right is the same diagram for $z(\varphi_m - \varphi_e) > 0$.

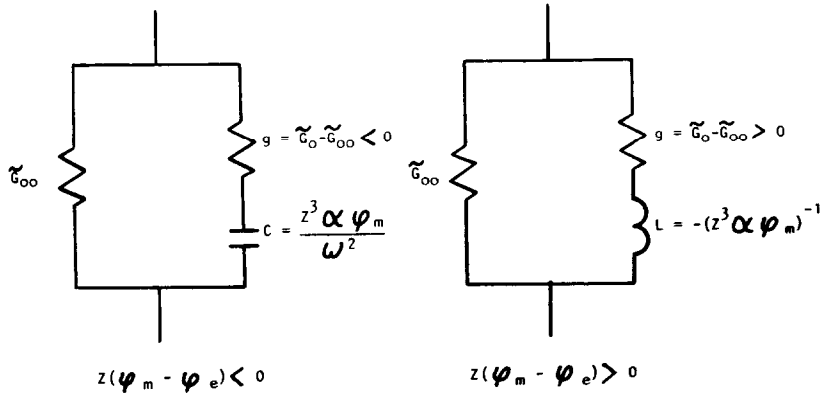

FIG. 2. The equivalent circuit representations for electrodiffusion membrane elements giving rise to the complex admittance plane properties shown in Fig. 1.

electrodiffusion model for ion transport predicts that near the resting potential, potassium ion movement should be associated with complex admittance properties containing an "anomalous" inductive element, while sodium movement should be associated with an "anomalous" capacitive reactance. These results are qualitatively consistent with the experimental behavior noted earlier, as well as the theoretical predictions of the small signal frequency domain approximation of the Hodgkin-Huxley equations.

Up to this point the spatial Fourier transforms $\tilde{G}_0(s)$ and $\tilde{G}_\infty(s)$ of $G_0(x)$ and $G_\infty(x)$ have been used exclusively. In a quantitative comparison between the Nernst-Planck formulations presented here and the only set of data available, the the Hodgkin-Huxley equations in the small signal approximation, it will be essential to have expressions for the integrated zero and infinite frequency conductances. From Eq. 20 and 21, $G_0(x)$ and $G_\infty(x)$ are easily integrated to give

$$G_{0m} = \left[\int_0^1 \frac{dx}{G_0(x)} \right]^{-1} = z^2 \tag{24}$$

and

$$G_{\infty m} = \left[\int_0^1 \frac{dx}{G_\infty(x)} \right]^{-1} = \frac{z^2 \varphi_m \beta}{\varphi_m - \varphi_e} \tag{25}$$

In accord with previous discussion, note that $G_{\infty m} \to z^2$ as $\varphi_m \to \varphi_e$ and $G_{\infty m} \to z^2$ as $\varphi_e \to 0$. Thus the anomalous impedance properties displayed by the electrodiffusion system disappear in the absence of ionic concentration gradients.

From the relations given above for $B(\omega)$, $G_0(\omega)$ and $G(\omega)$, the critical dimensionless frequency ω_c, defined as the solution of

$$B(\omega_c) = [G_\infty(\omega_c) - G_0(\omega_c)]/2$$

may also be calculated. In comparisons with e.g. the Hodgkin-Huxley parameters, however, ω_c is not as interesting as the dimensionless time constant of the system defined by $\omega_c \tau_c = 1$. When these determinations are carried through,

$$\tau_c(\varphi_m, \varphi_e) = \frac{[\varphi_m \beta(\varphi_m, \varphi_e)/(\varphi_m - \varphi_e)] - 1}{2z\varphi_m \alpha(\varphi_m, \varphi_e)}$$

results. It is easy to show that τ_c has a single maximum at $\varphi_m = \varphi_e$, and $\tau_c \to 0$ for $\varphi_m \to +\infty$. Qualitatively these results are as found for the τ_n of the

Hodgkin-Huxley formalism describing potassium current kinetics.

QUANTITATIVE COMPARISONS WITH DATA

The Hodgkin-Huxley [18] equations, in the small signal approximation [20], afford an excellent opportunity to compare the present predictions of the Nernst-Planck formulation of electrodiffusion theory with experimental data. It is well known (cf. [5]) that electrodiffusion theory is unable to match the known sodium conductance characteristics in the squid giant axon membrane. However, the potassium channel steady state conductance is at least semi-quantitatively consistent with the predictions of electrodiffusion theory, so I will concentrate my attention on the small signal approximation to the Hodgkin-Huxley expression for potassium current.

In the notation of Hodgkin and Huxley a small signal analysis of I_K yields the membrane equivalent circuit of Figure 2(b), where the circuit components are given by

$$G_K(V) = \bar{g}_K n_\infty \tag{26}$$

$$g_K(V) = \frac{4\bar{g}_K n_\infty^3 (V - V_K)\left\{ \frac{d}{dV}[\alpha_n(1-n)] - n_\infty \frac{d\beta_n}{dV} \right\}}{\alpha_n + \beta_n} \tag{27}$$

and

$$L_K(V) = \frac{1}{(\alpha_n + \beta_n) g_K(V)}. \tag{28}$$

The corresponding circuit values predicted from this study are

$$\bar{G}_K(V) = \frac{e^2 D_K \bar{N}_{iK}}{dkT} \frac{V + V_r}{V - V_{eK}} \frac{(\bar{N}_{dK}/\bar{N}_{iK}) - \exp[e(V+V_r)/kT]}{1 - \exp[e(V+V_r)/kT]}, \tag{29}$$

$$\bar{g}_K(V) = \frac{e^2 D_K \bar{N}_{iK}}{dkT} - \bar{G}_K(V), \tag{30}$$

and

$$\bar{L}_K(V) = -\frac{d^3 (kT)^2}{e^3 D_K^2 (\bar{N}_{iK} - \bar{N}_{dK})} \frac{1 - \exp[e(V+V_r)/kT]}{V + V_r}. \tag{31}$$

In Eq. 29 to 31 the theoretical results have been transformed back to dimensional form, and all potentials $\bar{\varphi}_m$ are expressed relative to the resting potential V_r. Thus $V = \bar{\varphi}_m - V_r$ and $V_e = \bar{\varphi}_e - V_r$.

For the purposes of computation take $T=6.3°C$, and $d=75$ Å. Data of Hodgkin and Huxley indicate $V_r \approx -60$ mV and $V_{eK} \approx -12$ mV. I assume $V_r = -60$ mV, and $V_{eK} = -11.2$ mV, thereby implying that $N_{iK}/N_{dK} = 20$, and thus $N_{iK} = 0.4$ mole/l if $N_{dK} = 0.02$ mole/l. The constant

$$G_0 = e^2 D_K \bar{N}_{iK} / dKT$$

appears in all three equations, (29)–(31), and if D_K has the units $cm^2\ sec^{-1}$, G_0 will have the value

$$G_0 = 1.95 \times 10^6 D_K \text{ mho/cm}^2.$$

No good independent estimate of D_K is available, so it is of interest to calculate the values of D_K which will bring the values for $\bar{G}_K$, $\bar{g}_K$, and $\bar{L}_K$ into agreement with the values predicted from the Hodgkin-Huxley equations:

Equations 26 through 28 give, at $V=0$ (i.e., the resting potential), $G_K(0) = 3.67 \times 10^{-4}$ mho/cm^2, $g_K(0) = 8.33 \times 10^{-4}$ mho/cm^2, and $L_K(0) = 6.43$ H cm^2. In order to obtain an exact correspondence between the value for $G_K(0)$ predicted by the Nernst-Planck and Hodgkin-Huxley analyses, D_K must be 10.66×10^{-10} cm^2/sec. With this value for D_K, $\bar{g}_K(0) = 1.71 \times 10^{-3}$ mho/cm^2 and $\bar{L}_K(0) = 1.77$ H cm^2. Thus there is a discrepancy in the $\bar{g}_K$ values by a factor of 2.05 and in the $\bar{L}_K$ values by a factor of 3.63.

TABLE 1

Predicted Values of $\bar{G}_K$, $\bar{g}_K$, and $\bar{L}_K$ at the Resting Potential for Three Different Potassium Diffusion Coefficient Values and the Corresponding Values Predicted by the Hodgkin-Huxley Equations.

$\bar{D}_K$ (10^{-10}cm^2/sec)	$\bar{G}_K(0)$ (10^{-4}mho/cm^2)	$\bar{g}_K(0)$ (10^{-4}mho/cm^2)	$\bar{L}_K(0)$ (H cm^2)
10.66	3.67	17.10	1.77
5.19	1.79	8.33	7.46
5.59	1.93	8.97	6.43
Hodgkin-Huxley	3.67	8.33	6.43

In Table 1 the values of D_K necessary to bring one of the three quantities being examined into exact agreement with values predicted by the Hodgkin-Huxley equations are listed. It would be possible to do a least

squares fit between Eq. 26 through 28 and 29 through 31 at $V=0$, simultaneously determining the best values of D_K, V_{eK}, and V_r, but there hardly seems to be any point in such an expenditure of time.

Mauro, Conti, Dodge, and Schor [20], Fig. 19(a) have plotted $G_K(V)$, $g_K(V)$, and $L_K(V)$ as obtained from the Hodgkin-Huxley equations (see Eq. 26 through 28) and the equations derived from this analysis, (29) through (31), show all of the same qualitative features.

One of the most interesting features of Table 1 revolves around the values of D_K necessary to bring the predicted values of $\bar{G}_K(0)$, $\bar{g}_K(0)$, and $\bar{L}_K(0)$ into agreement with their actual values. Using three different data the necessary values of D_K range between 5.19×10^{-10} and 10.66×10^{-10} cm^2/sec. The diffusion coefficient for K^+ in free solution at physiological concentrations and the same temperature range is some five orders of magnitude larger than these values, thus supporting the conclusions of Cole and Moore [12] and Cole [6] that K^+ diffusion with the membrane is much more restricted than in free solution. Cole's [6] estimate for D_K was 5×10^{-10} cm^2/sec.

I would like to express my warmest appreciation to Ms. Celia Lang for her meticulous typing of two versions of this paper and the drawing of figures.

REFERENCES

1 W. K. Chandler, R. Fitzhugh, and K. S. Cole, *Biophys. J.* **2**, 105 (1962).
2 H. Cohen and J. W. Cooley, *Biophys. J.* **5**, 145 (1965).
3 K. S. Cole, *J. Gen. Physiol.* **25**, 29 (1941).
4 K. S. Cole *Arch. Sci. Physiol.* **3**, 253 (1949).
5 K. S. Cole, *Physiol. Rev.* **45**, 340 (1965).
6 K. S. Cole, *Membranes, Ions, and Impulses*. Univ. of Calif. Press, Berkeley, Calif., 1968.
7 K. S. Cole, and R. F. Baker, *J. Gen. Physiol.* **24**, 771 (1941).
8 K. S. Cole and R. H. Cole, *J. Chem. Phys.* **9**, 341 (1941).
9 K. S. Cole and H. J. Curtis, *J. Gen. Physiol.* **22**, 37 (1938).
10 K. S. Cole and H. J. Curtis, *J. Gen. Physiol.* **22**, 649 (1939).
11 K. S. Cole and A. L. Hodgkin, *J. Gen. Physiol.* **22**, 671 (1939).
12 K. S. Cole and J. W. Moore, *Biophys. J.* **1**, (1960).
13 J. Cooley, F. Dodge, and H. Cohen, *J. Cell. and Comp. Physiol.* **66**, 99 (1965).
14 H. J. Curtis, and K. S. Cole, *J. Gen. Physiol.* **21**, 757 (1938).
15 B. Frankenhaeuser, and A. L. Hodgkin, *J. Physiol. (Lond.)* **137**, 217 (1957).
16 D. E. Goldman, *J. Gen. Physiol.* **27**, 37 (1943).
17 B. Hille, *Prog. Biophys. Mol. Biol.* **21**, (1970).
18 A. L. and A. F. Huxley, *J. Physiol. (Lond.)* **117**, 500 (1952).
19 A. L. Hodgkin, and W. A. H. Rushton, *Proc. Roy. Soc. Lond. B Biol. Sci.* **133**, 444 (1946).
20 A. Mauro, F. Conti, F. Dodge, and R. Schor, *J. Gen. Physiol.* **55**, 497 (1970).

21 W. Nernst, *Z. Phys. Chem. (Leipz.)* **2**, 613 (1888).
22 W. Nernst, *Z. Phys. Chem. (Leipz.)* **4**, 129 (1889).
23 M. Planck, *Ann. Phys. Chem. Nevefolge* **39**, 161 (1890).
24 M. Planck, *Ann. Phys. Chem. Nevefolge* **40**, 561 (1890).
25 J. Sandblom, *Biophys. J.* **12**, 1118 (1972).
26 S. Weidmann, *Experientia* **VI**, 1 (1950).